

OPTIMAL DEEP FEATURE MODEL SELECTION WITH WEIGHTED MULTI-SIMILARITY-BASED CONTENT-BASED IMAGE RETRIEVAL FRAMEWORK

G.KRISHNA RAJU¹, P.PADMANABHAM², A.GOVARDHAN³

¹Professor, Matrusri PG College, Hyderabad, MCA Department, India.

²Ex-Director Academics, Bharat Engineering College, Hyderabad, India.

³Professor, Rector JNT University Hyderabad, CSE Dept, India.

E-mail: ¹xxx@www.com, ²xxx@abc.com

ABSTRACT

The scheme of Content-Based Image Retrieval (CBIR) is developed for the process of retrieving of images on the basis of the visual elements defining the image content. Even though, it has certain complications of huge calculation problems such as scoring of the image similarity and feature extraction. The conventional feature extraction models only aim toward the high or low-level features and utilize few manmade features to minimize these gaps. It is required to establish a framework for feature extraction to minimize the gap without utilizing the manmade features from joining low and high-level features. The deep learning is considered as a very powerful tool for feature indication that can represent high and low-level information entirely. In this paper, new optimal deep learning model-based feature extractions for CBIR model are performed for retrieving the accurate images. In the training phase, diverse images are gathered from the standard database, which is used into Optimal Deep Feature Selection Model (ODFSM) by the deep learning models with VGG16, VGG19, Inception, Xception, Resnet50, Resnet101, Resnet 152, and Densenet for extracting the features. Here, the optimization in deep learning models takes place with the help of hybrid optimization algorithm known as Probability-based Coyote-Forest Optimization Algorithm (P-CFOA) for getting the efficient features. In the testing phase, the query images are given into optimal deep feature selection model for extracting the features of the query image. Then, the weighted multi-similarity is performed between the extracted features of database images and query image, in which the weights are optimized using the same P-CFOA. The database images with less weighted multi-similarity when correlated with extracted features of query image are retrieved finally. The simulation analyses are made to demonstrate the better efficiency of image retrieval through the optimal deep feature extractors.

Keywords: Content Based Image Retrieval, Multi-Similarity Function, VGG16, VGG19, Inception, Xception, Resnet, Densenet, Coyote-Forest Optimization, Optimal Deep feature Selection.

1. INTRODUCTION

In the speedy developing and methodology rushed era, the classification and recording of digital images get to be easy and viable broadly [9]. Hence, a large range of digital images are restored and upgraded online in large databases known as World Wide Web or in the clinical images database [10]. Similarly, a finding query on the basis of the images is highly needed. Since, these differ from the conventional databases by the kind of disorganized data recorded in them, renewed information recapturing techniques were established. There exist two kinds of models for image re-capturing known as text-based model and content-based model [11]. The text-based model

hangs on the physical indexing and the characteristics of the tagged words and annotations that defines the images for recapturing process [12]. The technique based on the annotation is obtained as a non-feasible recapturing method because of various reasons that are known to be tedious, incomplete, and high time-consuming and subjective in the physical annotation process [13]. Further, these allotted keywords will not define the images clearly, for example, various keywords can define a particular image and in the similar time a one-word keyword can define several images [14].

A CBIR is a connection point in-between the semantic gaps, which is defined as the variations in-between the human knowledge and computerized

knowledge discrimination [15]. The human knowledge is able to carry out the difficult optic discrimination at very speedy range but computerized systems will not [16]. In CBIR, the vision image elements are denoted as image features, which is gathered by utilizing automated feature collection techniques. Thus, the man-made invention is neglected [17]. The feature extraction process is systematically costlier and comprises of huge dimensionality and these techniques maintained to be remarkable domain [18]. A huge variety of investigations for reducing the complexity in these algorithms required to be noted [19]. The image elements are gathered from the database images and are restored as a database element of images. This process comprises of huge numbers of computations and considered as a complicated step to gather the image elements. The image element collection is gradually carried out based on the shape, texture, color features, in which low-range features denotes the image and then various techniques have been established [20]. The next step comprises of similarity metrics, which is an essential procedure as the results obtained is recaptured after the checking of similarity metrics. The user questionnaire image element is combined with the recorded element database that provides better available link based on the viewers query image [21]. Huge similarity linking techniques have been proposed which generally compute the available measures between the questionnaire image and database image.

With the development in deep learning models, a recapture technique on the basis of the successes in performing better than the conventional recapturing model that is based on the tagging of keywords and indexing of images, particularly if they find an image in huge database for combining the needed questionnaire images [22]. But, the deep learning model has degraded in performance and to become successful approach, they have to be combined with superior learning that needs a quoted dataset for the learning process and these quoted data represents the couple of inputs and quotes. This determines the clear output remarked with input that should be typically collected by a manual expert [23]. For a huge database comprises of several images, there exist certain limitations of the content-based models [24]. Hence, enhanced deep learning models are needed to make essential backbone to this gap for recapturing the images because of its ability to process new data and create the interior features indication of it by its several linear levels of distraction to give huge image concept indication of image eventually [25]. This issues in CBIR and deep learning progression gives

motivation to develop a new CBIR scheme by utilizing deep learning technique.

The major highlights of the developed CBIR scheme are briefed below:

- To establish an improved CBIR model with weighted multi-similarity function with deep feature extraction model based on three similarity metrics such as Euclidean, Jaccard and cosine for improving the retrieved image efficiency.
- To select the best optimal feature extraction model using the developed algorithm from the set of deep learning models like VGG-16, VGG-19, Inception, Xception, ResNet-150, ResNet-101, ResNet-152 and Densenet to generate the effective deep features for CBIR model.
- To retrieve the accurate images on the basis of query images by utilizing the weighted multi-similarity function using Euclidean, Jaccard and cosine similarity metrics with the weight optimization to enhance the retrieval performance using developed P-CFOA algorithm.
- To develop a new P-CFOA model for the process of selection of optimal deep feature models in the training phase among the eight deep feature extraction models and also for optimizing the three weights integrated with the multi-objective functions to elevate the accuracy of image retrieval.
- To evaluate the effectiveness of developed CBIR scheme between the retrieved and query images by comparison with conventional CBIR approaches with standard analysis measures.

The remaining portions of the developed scheme are briefed as follows. The section II discusses the available investigation works. The section III recommends the gathering of dataset images and developed CBIR model description. The section IV suggests the implementation of developed P-CFOA model along with multi-similarity function. The section V proposes selection of optimal deep feature model by considering eight models along with weight functions. The section VI analyses the experimentation results. The section VII provides conclusion of the paper.

2. LITERATURE SURVEY

6.1 Related Works

In 2017, Liu *et al.* [1] have presented an efficient image retrieval technique by the combination of large-level elements from

Convolutional Neural Network (CNN) model and minimum-range elements from Dot-Diffused Block Truncating Coding (DDBTC). The minimum-range features such as color and texture were built by quantization histogram of the similar vector from the DDBTC map, low and high quantizes. Contrarily, large-range features from CNN have been efficiently seized the human discrimination. By the fusion process of DDBTC and features of CNN, the expanded code-book on the basis of deep learning were created by utilizing the proposed codebook with two-layers, minimization of dimension and similar weighting to enhance the complete range of retrieval. Two measures, recall rate and average range of precision were processed to analyze several datasets. As discussed in the experimentation results, the developed scheme attained greater performance compared to the other traditional methods on the basis of retrieval range.

In 2017, Swati *et al.* [2] have proposed a deep-CNN based on the VGG-19 for the process of extraction of features and the fastened learning measures were applied for determining the similarity of database and query image. Moreover, they considered transfer learning and established a block-wise approach for the process of fine tuning to improve the retrieval rate. The expanded analyses were carried out on a commonly presented dataset known as CE-MRI that comprised of three kinds of brain tumors monitored from 234 patients along with the image count of 3064. The technique was highly non-specific because they will not utilize any manmade elements, and it needed low pre-processing images. Thus, the model has achieved average validity while carried out with CE-MRI datasets. In 2019, Mustaficet *al.* [3] have showed a novel scheme for enhancing the performance of the CBIR by utilizing deep network. The major aim of the technique was the learning of distance element by utilizing the deep networks and transfer learning model. The pre-trained neural networks available for categorization of images were utilized as bias. The techniques were evaluated with the commonly available networks. The gathered experimentation results were compared with other conventional approaches.

In 2021, Ahmed *et al.* [4] have proposed an efficient CBIR on the basis of CNN with the applications gathered from the augmented data. In the CNN, the generation of feature elements was carried out by utilizing trained CNN without entirely joined layers to obtain an enhanced result than the problems of over-fitting in CNN. The training of data augmentation technique was carried out to extent the images from the training. The

performances of considered CNN were improved by utilizing meta-heuristic optimization during the phase of training. After that, the CNN were utilized as a classifier to categorize the developed CNN in the region of training. Then, it was analyzed by utilizing arbogreen and Swiss mountain dataset. The experimentation results represented that the CNN has attained minimum loss for retrieval.

In 2022, Agrawal *et al.* [5] have proposed an effective Content-based Medical Image Retrieval (CBMIR) for inducing the early identification and categorization of lung diseases on the basis of the X-ray images. The developed CBMIR system was implemented on the prediction power models for the determination and categorization of disease elements by utilizing the transfer learning models. The experimentation results of the dataset showed that the proposed scheme attained an enhancement in terms of validity, averaging and precision measures. Also, developments were monitored across the area of precision-recall curve in all classes.

In 2021, Desai *et al.* [6] have improved a robust system that generated and executed in an efficient manner. A CBIR system has been implemented effective gadget for image retrieval, where the viewers submitted their inquiry to the computerized system to permit the user to collect the required image from the gathered images. Further, the need of web enhancement and transfer networks were presented to viewers. They established an efficient deep learning scheme on the basis of CNN and Support Vector Machine (SVM) for speedy recapturing of images. The experimentation results described the efficiency of the system. In 2021, Tuyet *et al.* [7] have proposed a renewed technique for CBMIR on the basis of deep learning and salient phases. The proposed technique has two phases: an offline phase to collect the common images and an online phase for CBMIR database. In the first phase, they collected the common features of clinical images on the basis of texture, shape and intensity and elements collected from deep learning was placed in salient degradation. Then, they made online session for CBIR in database. The viewers have given images for questioning as input and the computerized system will recapture in the highly identical images by conducting the process of similarity comparison along with the storage of code words values of features gathered in the first phase. The analysis of the developed model was on the basis of the validity and values of recall. The dataset comprised of 5 counts of group of images along with their worth differentiating from minimum to maximum. By considering the better medical image quality,

the accuracy attained higher when comparison with the averaging values using various techniques.

In 2020, Yoshi *et al.* [8] have proposed a deep learning technique for CBIR by utilizing the multi-phase contrast improved CT images. They utilized deep-CNN to collect the spatial elements from the CT images and compared to the minimum-and medium-level elements. The large-level elements were collected by DCNN, which remarkably enhanced the recapture accuracy. The efficiency of the proposed model was described through experimentations with the multi-level datasets.

2.2 Problem statement

There exists a huge number of research based on the CBIR. A lot of work has been done for the labeled images. These methods are costly, time-consuming and less feasible for various applications. Hence, the challenges involved in existing content-based image retrieval are represented in Table.1. DL-TLCF [1] can examines huge variety of datasets and it is robust and effective candidate for the image retrieval application. CBIR approaches [2] can utilize block-wise fine-tuning strategy to enhance the retrieval

performance but it requires only MR images for the retrieval process. Device finger printing algorithm [3] can utilize the geo-location data, which enhances the finger print accuracy but it drastically improves the legitimacy of the fingerprints generated. CNN [4] has more learning features for the classification of high-resolution images but There exist over fitting issues during pre-training and it comprises of deep features, which is difficult to learn. CBMIR systems [5] can enables early detection of disease by utilizing the X-ray reports and this system maintains high-level image visuals but it does not process model with a larger dataset with more subclasses. CNN and SVM [6] can handle huge number of datasets at once and it reduces the time required for image retrieval but it has exploding gradient issues during processing. CNN [7] can applies the models of larger data sets with thousands of contents and it uses multitask learning to solve more problems but it doesn't focus on the early cooperation before classification and the max-pool involved in this makes CNN significantly slower. APHA [8] has no security defects and it provides suitable solutions for security protection of data but it has slight design defects, which affect the performance quality.

Table 1: ThePros and Cons of Content-Based Image Retrieval

Author [citation]	Methodology	Features	Challenges
Liu <i>et al.</i> [1]	DL-TLCF	<ul style="list-style-type: none"> It is robust and effective candidate for the image retrieval application. It examines huge variety of datasets. 	<ul style="list-style-type: none"> It does not neglect the irrelevant images effectively. It does not extract highly complicated deep features from the images.
Swati <i>et al.</i> [2]	CBIR approach	<ul style="list-style-type: none"> It uses block-wise fine-tuning strategy to enhance the retrieval performance. It requires only MR images for the retrieval process. 	<ul style="list-style-type: none"> It does not use any hand-crafted features, so the computational cost becomes high.
Mustaficet <i>al.</i> [3]	Device finger printing algorithm	<ul style="list-style-type: none"> It uses the geo-location data, which enhances the finger print accuracy. It drastically improves the legitimacy of the fingerprints generated. 	<ul style="list-style-type: none"> In this, the usage of different web-clients from same web-machine is not possible. It does not have hardware parameters.
Ahmed <i>et al.</i> [4]	CNN	<ul style="list-style-type: none"> It has more learning features for the classification of high-resolution images. 	<ul style="list-style-type: none"> There exist over fitting issues during pre-training. It comprises of deep features, which is difficult to learn.
Agrawal <i>et al.</i> [5]	CBMIR systems	<ul style="list-style-type: none"> It enables early detection of disease by utilizing the X-ray reports. This system maintains high-level image visuals. 	<ul style="list-style-type: none"> It does not process model with a larger dataset with more subclasses.
Desai <i>et al.</i> [6]	CNN and SVM	<ul style="list-style-type: none"> It can handle huge number of datasets at once. It reduces the time required for image retrieval. 	<ul style="list-style-type: none"> It has exploding gradient issues during processing.
Tuyet <i>et al.</i> [7]	CNN	<ul style="list-style-type: none"> It applies the models of larger data sets with thousands of contents. It uses multitask learning to solve more problems. 	<ul style="list-style-type: none"> It doesn't focus on the early cooperation before classification. The max-pool involved in this makes CNN significantly slower.
Yoshi <i>et al.</i> [8]	APHA	<ul style="list-style-type: none"> It has no security defects. It provides suitable solutions for security protection of data. 	<ul style="list-style-type: none"> It has slight design defects, which affects the performance quality.

3. ENHANCED FRAMEWORK FOR CBIR USING OPTIMAL DEEP FEATURE SELECTION MODEL

monuments, animal and mountains, elephants, foods, villages, flowers, bus, people and dinosaurs in Africa.

3.1 CBIR Dataset

The developed CBIR model collects the query and input images from two standard datasets for the process of experimentation, which was explained below.

Dataset-1 (“corel_images”): The images needed for retrieval is gathered from the link: “<https://www.kaggle.com/datasets/elkamel/corel-images>: access date: 05-07-2022”. It comprises of 10 counts of concept groups, in which each one of them composes of 100 images. For each group of concepts, the image is categorized into 90 training images and 10 testing images. The available 10 count of groups in the dataset are beaches, snow,

Dataset 2 (“VisTex database”):The required images are gathered from the link: “<http://vismod.media.mit.edu/pub/VisTex/>: access date: 05-07-2022”. It comprises of several classes along with bark of 3 scenes, granite, water, marble, wood of 3 scenes, wall, brick, pebbles, floor of 2 scenes, carpet with 2 scenes, fur, glass with 2 scenes, knit, upholstery, plaid and corduroy.

Hence, the database images collected are represented as D_x , where $x = 1, 2, \dots, X$ and the total image count is represented as X and the query images collected are denoted as q_x , where $x = 1, 2, \dots, X$. Few of the gathered query images are represented in Fig. 1.

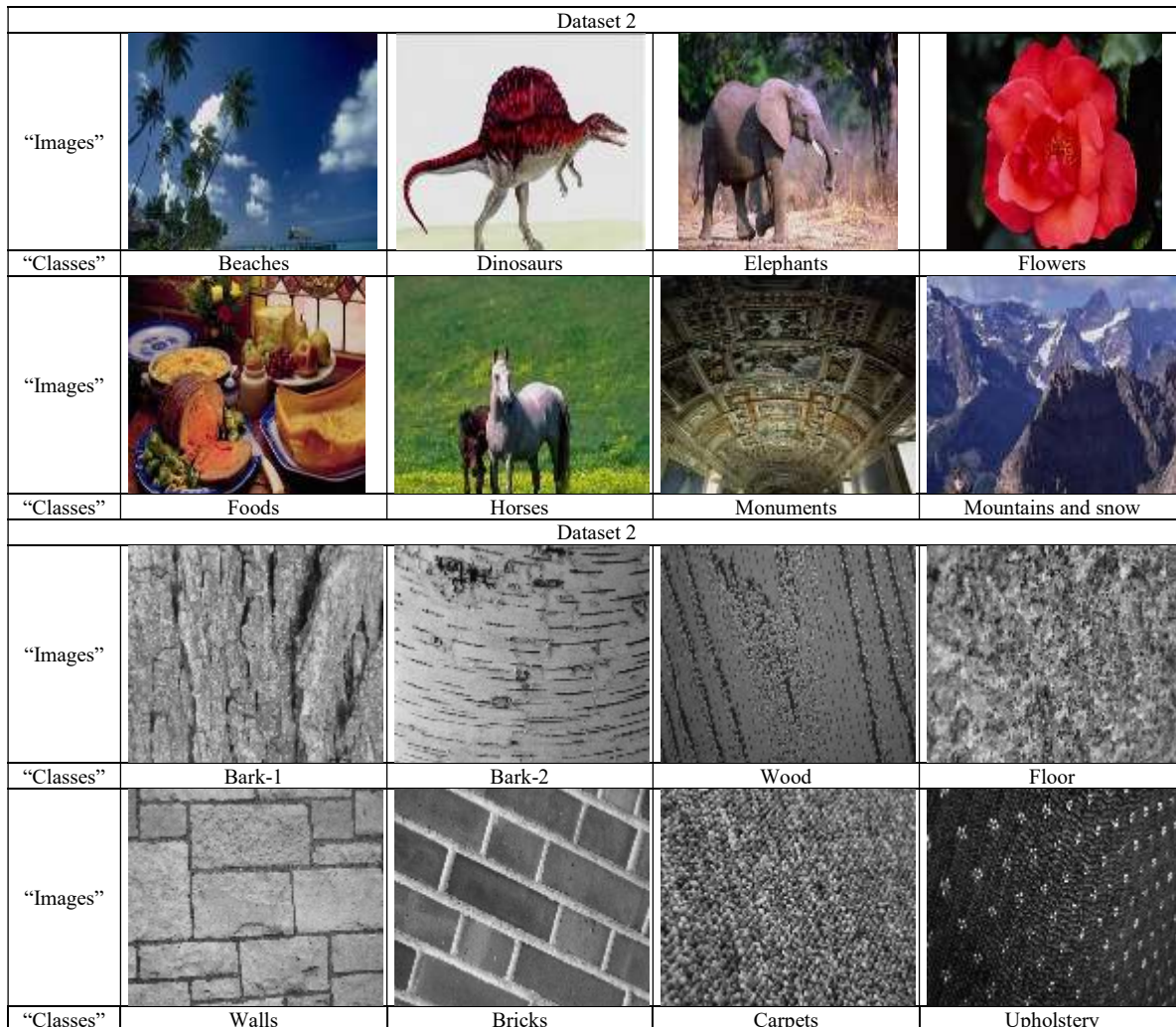


Figure 1: Samples of gathered query images from dataset 1 and dataset 2

3.2 Proposed System Framework and Description

The CBIR is considered as a newly developed research platform for monitoring the complications available in the studies as it was evaluated by the visual contents by utilizing the query image. In the CBIR approach, the issue of attaining same images with larger accuracy is now complicated because of its huge count of database images. The conventional findings of images are carried out by using the queries in text form. The “image query-based retrieval system” requires recapturing of images with high similarity and with validity for annotation of the complete images. Furthermore, it is difficult to find out the annotations for the application of particular image to attain larger accuracy in image retrieval. The CBIR model supports in recapturing or finding the required

images from the available database, although, it is a difficult issue because of its processing of huge-scale images. The basic need of the common image re-capturing system is to sequence the images by utilizing the “visual semantic relationship with the query provided by the user”. Few search engines available in the internet attains the required images by using text-based schemes but they are not feasible and applicable for manual labeling concept to achieve of traditional large-scale images along with millions of images considered. Hence, the multi-similarity function is required in the model for retrieving the large-scale images in datasets considered. Thus, a developed CBIR model along with the multi-similarity function is established for retrieving the large-scale query images. The diagrammatic representation of developed CBIR model is depicted in Fig.2.

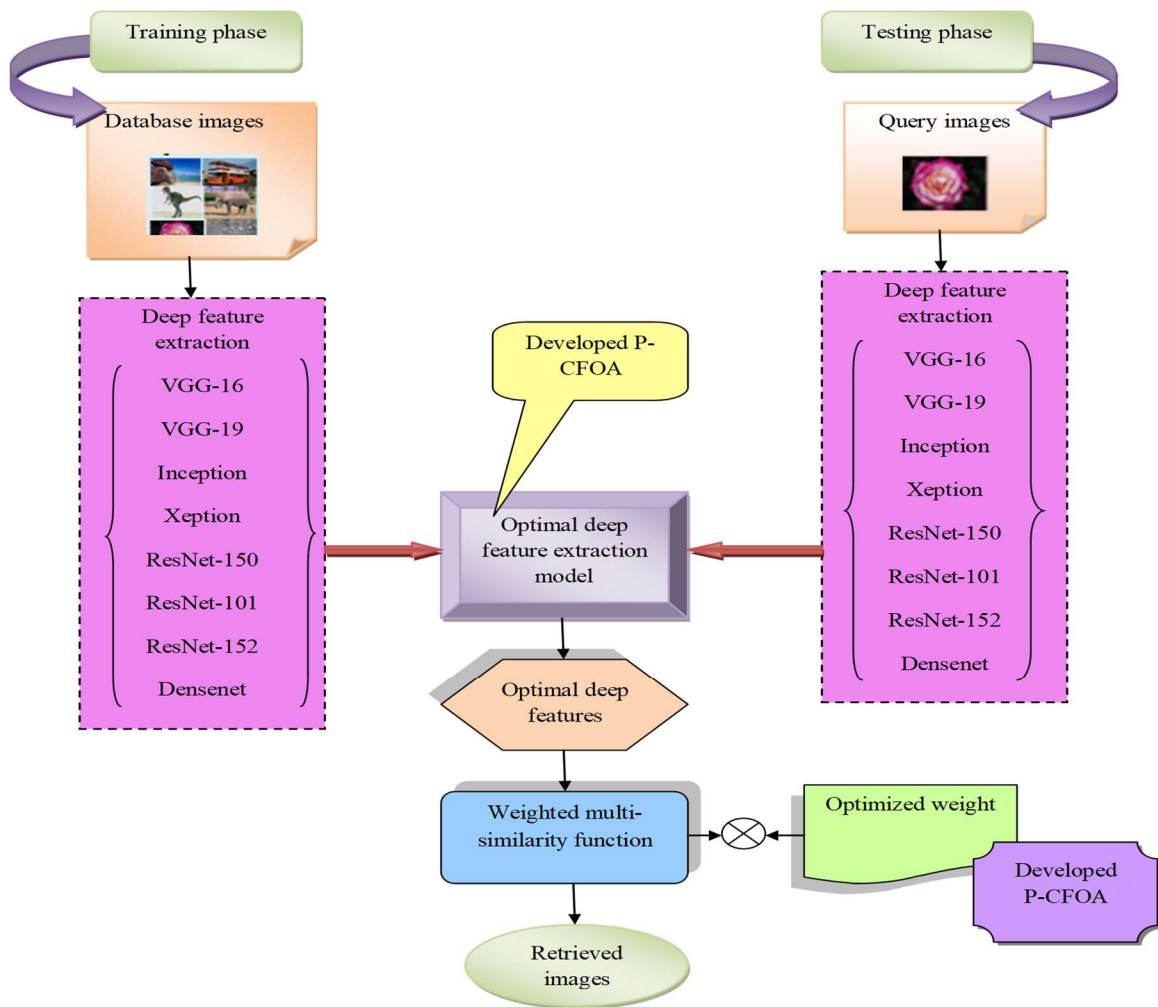


Figure 2: Weighted multi-similarity-based CBIR model with deep feature extraction model

A new CBIR scheme is established with deep feature extraction model on the basis of multi-similarity function. The developed framework follows deep feature extraction model, optimal weighted feature selection, the computation of multi-similarity and image retrieval. At first, in the training phase, the database and the query images are provided to the process of deep feature extraction model with the developed ODFSM that is integrated by utilizing various models such as VGG-16, VGG-19, Inception, Xception, ResNet-150, ResNet-101, ResNet-152 and Densenet. From the eight considered models, the best model is selected as the final deep feature model by utilizing developed P-CFOA. The calculation of multi-similarity function is carried out for both database and query images along with the similarity measures such as “cosine, Euclidean and Jaccard” metrics. For each similarity measure the weight function is multiplied to obtain weighted-multi-similarity function, in which the weights are optimized by using developed P-CFOA. Finally, the retrieval of image comprises of minimum similarity between the database and query images are carried out.

4. IMPLEMENTING A NOVEL WEIGHTED MULTI-SIMILARITY FUNCTION FOR CBIR

6.1 New Weighted Multi-similarity Function

The comparison of optimal weighted features obtained from the query images q_x and the database images D_x are carried out into multi-similarity function for obtaining query-based images. In the investigation platform of CBIR, the finding of similarity along with the typical measures plays a vital role that supports in determining the visual identities on the images in database. Hence, the recapturing outcome was not obtained as an individual image but in group of images. Usage of several identity measures provides reduction in the efficiency of the image recapturing schemes. Hence, there arises a requirement to determine the suitable measure for CBIR model. During the adoption of smaller range for the measured distance, the query images are considered moreover equal to the database images. The identification with three metrics of distance known as Jaccard, cosine and Euclidean similarity measures are utilized for determining the similarities on the database features and query-related images. Thus, the weighted multi-similarity function WMS is computed on the basis of Eq. (1).

$$WMS = (W_1 * Co) + \left(W_2 * \left(\frac{1}{ds} \right) + (W_3 * Ja) \right) \quad (1)$$

Here, the terms W_1, W_2 and W_3 indicated the optimized weights and Co denotes cosine similarity and ds indicates Euclidean distance and Ja represents the Jaccard similarity. Hence, the similarity of cosine is defined as the “measures the similarity between two vectors of an inner product space and it is measured by the cosine of the angle between two vectors and determines whether two vectors are pointing in roughly the same direction” as indicated in Eq. (2) below.

$$Co(E_s^*, U_s^*) = \frac{E_s^* \cdot U_s^*}{\|E_s^*\| \cdot \|U_s^*\|} \quad (2)$$

Then, the Euclidean distance is defined as “the distance between two feature vectors” as shown in Eq. (3) below.

$$ds(E_s^*, U_s^*) = \sqrt{\sum (E_s^* - U_s^*)^2} \quad (3)$$

Moreover, the Jaccard similarity is explained as “the size of the intersection divided by the size of the union of two lists” and it is typical metrics of statistics that defines “the similarity between two feature sets based on their intersection”, which are computed in Eq. (4).

$$Ja(E_s^*, U_s^*) = \frac{|E_s^* \cap U_s^*|}{|E_s^* \cup U_s^*|} \quad (4)$$

Thus, the multi-similarity function on the query-based images and the image of database attains retrieval images.

6.2 Proposed P-CFOA Model

In the CBIR framework, the low-level feature of the images does not have the capacity to interpret and describe the context of the image semantically. There also exists un-serviceability for the typical users as they need to give query in image format. Hence, for minimizing these odds, a new hybrid optimization algorithm known as P-CFOA is established for obtaining the optimal feature models among the eight deep feature extraction models and for weight optimization in the weighted multi-similarity function. The developed P-CFOA enhances the retrieval performance of the images. It is implemented based on the concept of COA and FOA. In the proposed P-CFOA algorithm, the parameter like probability of leaving pack P_{lev} in the conventional COA algorithm is updated in terms of area limit and transfer rate-based concept and it is mathematically derived in following Eq. (5).

$$P_{lev} = \left(\frac{are_{lim}}{tra_{ra}} * (ch_{le})^2 \right) \quad (5)$$

Here, the term are_{lim} denotes area limit, tra_{ra} represents transfer rate and ch_{le} indicates chromosome length. The probability of leaving pack P_{lev} is used for determining the position update procedure by deriving the condition ($P_{lev} \geq 0.5$). If this condition ($P_{lev} \geq 0.5$) is satisfied, then the position update is performed with the procedure of COA or else with the procedure of FOA.

COA [26] is inspired from the nature of the coyote animals. This algorithm is clearly based on the population on the coyote limitations. The coyote population CP comprises of packs count and each and every pack comprises of CN coyotes. The total count of the coyotes present in every pack denotes the population present in optimization problem. The adaption of optimality to each and every social condition defines the solution of optimality problem. These constrains in sociality denotes the “d-space” variables present for the making decision of optimization issues. The condition of sociality of the coyote $soco$ in the n^{th} pack at i^{th} time instance is represented by $soco_d^{n,i}$. This coyote limitation denotes the decision variables \bar{Y} of a particular global optimization issues. It is derived as shown in Eq. (6) as follows:

$$soco_d^{n,i} = \bar{Y} = (y_1, y_2, \dots, y_c) \quad (6)$$

The initial sociality condition is generated randomly for every coyotes d^{th} distance of n^{th} pack at instant i^{th} and l^{th} dimension at the level of upper and lower bounds, lb_l and ub_l of the decision variables indicated below Eq. (7):

$$soco_d^{n,i} = lb_l + re_l \times (ub_l - lb_l) \quad (7)$$

Here, the term re_l denotes the actual random number presented in the range of $[0, -1]$, which is created by utilizing a uniform probability.

The objective function is gathered by analyzing the conditions of the coyote to the present decision variables as shown below in Eq. (8).

$$F_d^{n,i} = f(soco_d^{n,i}) \quad (8)$$

The algorithm randomly upgrades the position of the groups. Apart from that, the candidate upgrades their location by leaving their packs to other. Hence, the probability of leaning pack P_{lev} is updated in terms of area limit and transfer rate in the proposed algorithm, whereas in the conventional algorithm, it is updated with the random variables.

Then, the term “alpha”, which is considered as the best solution for the optimization problem under global conditions is computed by Eq. (9).

$$\text{alpha}^{n,i} = \left\{ \text{soco}_d^{n,i} \mid \arg_{d=(1,2..C_N)} \min f(\text{soco}_d^{n,i}) \right\} \quad (9)$$

Then, the upgrading of social conditions $ne_{sod}^{n,i}$ of coyotes are depending on the couple of factors such as alpha influence δ_1 and cultural tendency influence δ_2 . The influence δ_1 is considered as the variations from the internal random coyote rc_1 to the alpha coyote. Then, the influence δ_2 is taken as the variations from the pack’s random coyote rc_2 to the cultural tendency, which is derived in Eq. (10) and Eq. (11), respectively.

$$\delta_1 = \text{alpha}^{n,i} - \text{soco}_{rc1}^{n,i} \quad (10)$$

$$\delta_2 = \text{cul}^{n,i} - \text{soco}_{rc2}^{n,i} \quad (11)$$

$$ne_{sod}^{n,i} = \text{soco}_d^{n,i} + r_{n1}\delta_1 + r_{n2}\delta_2 \quad (12)$$

Here, the term $cul^{n,i}$ denotes the cultural tendency of the pack. The terms r and r denotes the number of random variables, which are uniformly distributed in the range of $[0, -1]$. The new value of the objective function is analyzed by the renewed social conditions as indicated in Eq. (13).

$$ne_d^{n,i} = f\left(ne_{soco_d}^{n,i}\right) \quad (13)$$

Then, the new social condition $ne_{soco_d}^{n,i}$ decisions is taken based on the objective function value as indicated in Eq. (14) below.

$$soco_d^{n,i+1} = \begin{cases} ne_{sod}^{n,i}, ne_d^{n,i} \leq F_d^{n,i} \\ \text{soco}_d^{n,i} \text{ otherwise} \end{cases} \quad (14)$$

For maintaining the size of the pack in static condition, COA calculates the ages of every coyotes placed inside the pack using Eq. (15).

$$pu_l^{n,i} = \begin{cases} \text{soco}_{rc1,l}^{n,i}, \text{rand}l \leq l = l_1 \\ \text{soco}_{rc2,l}^{n,i}, \text{rand}l \geq l = l_2 \\ R_l \text{ otherwise} \end{cases} \quad (15)$$

Here, the term R_l denotes a random number placed inside the bound of the decision variable. Then, the scatter and association probabilities are computed by the following Eq. (16) and Eq. (17).

$$Ps = \frac{1}{c} \quad (16)$$

$$Pa = (1 - Ps)/2 \quad (17)$$

Here, the term Ps denotes the scatter probability and Pa indicates the association probability.

FOA [27] is inspired by nature on the basis of the trees present in forests. Moreover, a tree with a best position comprises of greater chance of the survival, when compared with the other trees.

Initialization: This algorithm is capable to resolve non-linear problems and similar to other available algorithms, that is initialized by the random populations. Each separate variable of the population is considered as a tree. Every individual tree is considered as an array with length of $1 * (Mvar + 1)$ as described in Eq. (18) below. Each individual tree comprises of M – dimension problem,

$$\text{tree} = [\text{age}, u_1, u_2, \dots, u_{Mvar}] \quad (18)$$

Here, the term $Mvar$ denotes the variable count, age represents the individual’s age and u_1, u_2 indicates the problem variables. From, the above equation, it is analyzed that every individual tree comprises of an age component initialized as zero.

Algorithm 1: Proposed P-CFOA
Initialize the population
Update the parameters of COA such as Pa, Ps
Update the parameters u_1, u_2
Compute the value of fitness F
while ($i_t \leq i_{\text{max}}$)
for $i = 1$ to M
Update the probability of leaving pack P_{lev}
if ($P_{\text{lev}} \geq 0.5$)
Position update of the solution Eq. (15) and Eq. (16) using COA
else
Position update of the solution Eq. (17) using FOA
end if
end for
end while
Obtain the best solution
end

Seeding of trees: The algorithm comprises of global and local seeding. Local seeding is defined as the investigation structure and global seeding is for utilization. The local seeding is mainly applicable for trees with zero components. Finally, in this phase, a newly created tree is added to the forest. All the trees are sequenced based on their fitness value and the tree comprises of greater lifetime than the considered lifetime that is neglected and added to the candidate solution.

Limiting the population: To limit the size of the population, the parameter known as “lifetime” is considered, which represents the maximum age of the tree for its survival. The parameter known as “area limit” is considered as the count of maximum trees available in the forest.

Updating the best tree: The trees are sequenced on the basis of the fitness value, the best age of the tree is calculated and upgraded to zero due to its age limiting problem. The local seeding can be utilized for the tree, which comprises of zero value and it will support in optimizing the better solution.

The Fig.3 represents the flow chart of the developed P-CFOA.

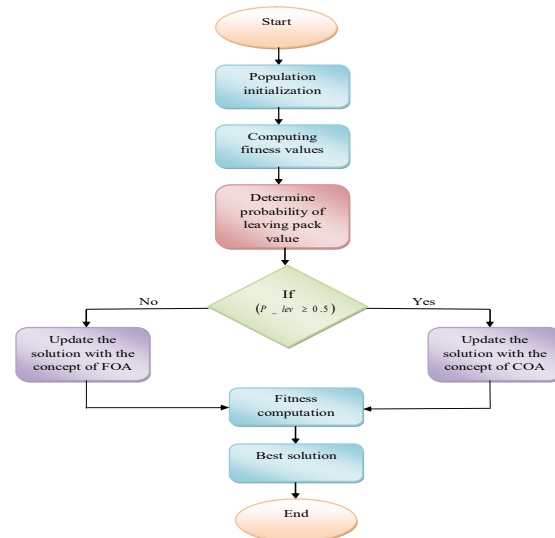


Figure 3: Flowchart of developed P-CFOA

6.3 Objective Function for Proposed CBIR System

In the proposed CBIR framework, the database and query images are considered for the retrieval. Hence, for removing the unwanted features from the images and to enhance the quality of the image for effective retrieval, the developed ODFSM is utilized. In this, eight models are considered namely VGG-16, VGG-19, Inception, Xception, ResNet-150, ResNet-101, ResNet-152 and Densenet. The eight deep feature extraction model is used for processing with developed P-CFOA for obtaining optimal deep feature model. From the obtained features, the best features are selected by conducting the comparative analysis between the features obtained from the database and query images. The comparative analysis is done by considering three similarity measures known as Jaccard, cosine and Euclidean. Then, the weighted multi-similarity function is utilized on the selected deep features. It considers 10 count of population and the model selection lies in-between the range of [1,8] and the weight function lies in-between the range of [0.01, 0.099]. Then, the objective function for the developed CBIR model is computed on the basis of following Eq. (19).

$$\text{OBfn} = \underset{(FM_z^{\text{best}}, W_1, W_2, W_3)}{\text{argmin}} \left(\frac{1}{\text{men}(f1s) + \text{men}(\text{pre}) + \text{me}(\text{rec})} \right) \quad (19)$$

Here, the term FM_z^{best} denotes best deep extracted model feature, W_1, W_2 and W_3 indicates the

optimized weights of multi-similarity function, $men(f1s)$ indicates F1-score mean, $men(pre)$ represents the mean of precision, $me(rec)$ indicates the mean of recall, which are computed by using Eq. (20), Eq. (21) and Eq. (22) as shown below.

Precision: It is defined as “the ratio of positive observations that are predicted exactly to the total number of observations that are positively predicted”.

$$pre = \frac{tr^{pos}}{tr^{pos} + fa^{pos}} \quad (20)$$

Recall: It is “the number of true positives, which are recognized exactly”.

$$rec = \frac{2tr^{pos}}{tr^{pos} + fa^{neg}} \quad (21)$$

F1-score: It is “the harmonic mean between precision and recall. It is used as a statistical measure to rate performance”.

$$F1s = \frac{2tr^{pos}}{2tr^{pos} + fa^{pos} + fa^{neg}} \quad (22)$$

Here, terms tr^{pos} , tr^{neg} , fa^{pos} , fa^{neg} refer to the “true positives, true negatives, false positives, and false negatives,” respectively.

5. OPTIMAL DEEP FEATURE SELECTION MODEL FOR ENHANCED CBIR

5.1 Deep Feature Extraction Models

This network obtains the deep features FE_t^{deep} from collected database images D_x , and from the query images q_x . In the CBIR framework, the optimized deep feature extraction is carried out for collecting the most relevant features for improving the accuracy of the proposed scheme. For this process, the VGG-16 [30], VGG-19 [30], Inception [31], Xception [32], ResNet-150 [33], ResNet-101 [33], ResNet-152 [33] and Densenet [34] networks are utilized as the deep feature extraction.

VGG 16 [30]: The VGG-16 comprises of three layers known as pooling layer, convolution layer and entirely-joined layers. It takes place of total count of 16 layers other than the pooling layers. It comprises of an enhanced network structure. In this, the size of the input image is allotted in the range of “224 × 224pixels”. The filter size of the considered image is chosen as “3 × 3pixels”. The layer of the output in the VGG-16 is known as

softmax and it comprises of an activation function and it provides the probability values of every classes. The extracted deep feature from VGG-16 is denoted as $FE_s^{deepVGG16}$.

VGG-19 [30]: It comprises of total count of 19 layers, out of those 16 layers are convolutional and 3 layers are entirely connected. The filter is utilized in the convolutional layer to minimize the parameter count as deep networks. The size and shape of the chosen filter in this model is “3 × 3pixels”. The steps involved are of two numbers and also the high pooling layer is utilized. The VGG-19 comprises of totally 138 million parameters for the process of computations. The extracted deep feature from VGG-19 is denoted as $FE_p^{deepVGG19}$.

Inception [31]: It is a type of convolutional neural network approach. It comprises of enormous convolution and huge pooling procedures. In the final level, it comprises of an entirely connected network and it is pre-trained by utilizing the ImageNet dataset. The extracted deep feature from inception is denoted as $FE_g^{deepInc}$.

Xception [32]: This model is formulated under the motivation from the inception architecture. It comprises of separate convolutions stacks in the depth wise parameters. Xception approaches have utilized reverse order parameters. Initially, the 1 × 1 convolutions process is applied along the input phase and then it provides the depthwise convolution processing. The xception model comprises of 14 modules including 30 layers of convolutions. The input image of the approach is considered in the size of 299 × 299 × 3 and it is altered to include a single pooling layer on the basis of the global average, one entirely joined layer and a layer of output sequenced on the basis of the categorization. In the entirely joined layers, the dropout layers, normalization layers and L2 regulations are utilized. The extracted deep feature from xception is denoted as $FE_h^{deepXep}$.

ResNet-150 [33]: It is an enhanced version of the CNN. The ResNet provides shortcut in-between the layers to resolve an issue. It also neglects the dispersion range that takes place during the complex formation of network. Additionally, the “bottle neck blocks” are utilized to make the speedy learning process in the mode of the ResNet. The “ResNet 150” is a 150-layer trained model for the image identification. The extracted deep feature from ResNet-150 is denoted as $FE_e^{deepRN150}$.

ResNet-101 [33]: It comprises of 101 sections of layers because of the presence of ResNet building blocks, which are stacked. The network comprises of pre-trained rich elements representations for a huge variety of images. The input sizes of the obtained images are 224×224 . The extracted deep feature from ResNet-101 is denoted as $FE_k^{deepRN101}$.

ResNet-152 [33]: ResNet-152 comprises of 152 sections of layers because of the presence of ResNet building blocks, which are stacked. It has the capability to load pre-trained model of the network, which is trained on greater than a million count of images obtained from the database known as ImageNet. The extracted deep feature from ResNet-152 is denoted as $FE_k^{deepRN152}$.

DenseNet [34]: In the conventional CNN, every layer is literally inter-connected with information, which forces the network to penetrate deeper and wider as it may cause issues related to the exploding or disappearing of gradient. Then, the DenseNet alters the scheme through concatenating every feature maps gradually by neglecting the process of summation of the available output feature map from every prior layer as represented in following Eq. (23), Eq. (24) and Eq. (25).

$$FE_{li} = L_{li}(v_{1i-1}) \quad (23)$$

$$FE_{li} = L_{li}(v_{1i-1}) + (v_{1i-1}) \quad (24)$$

$$FE_{li} = L_{li}([v_0, v_1, v_2, \dots, v_{li-1}]) \quad (25)$$

Here, the term li represents the index layer and L denotes the non-linear operation and v_{li} denotes the feature of li^{th} layer. The extracted deep feature from densenet is denoted as $FE_{li}^{deepDen}$. From these 8 features the best deep feature model is extracted for database and query image and is represented as D_o^{besfea} and q_u^{besfea} , respectively.

5.2 Optimal Deep Feature Selection Model

The suggested CBIR framework establishes a novel optimal weighted feature selection process, in which the optimal feature models are chosen by utilizing developed P-CFOA. Here, from the collected set of model features such as $FE_s^{deepVGG16}$, $FE_p^{deepVGG19}$, $FE_g^{deepInc}$, $FE_h^{deepXep}$, $FE_e^{deepRN150}$, $FE_k^{deepRN152-101}$ and $FE_{li}^{deepDen}$, the best featured model are selected by utilizing developed P-CFOA. This process of selecting optimal deep feature

model helps in determining the most remarkable feature model. It also helps in minimizing the time consumption of training, obtaining enhanced accuracy, neglecting the unwanted features and reducing the over-fitting issues. The optimally selected feature models by utilizing the P-CFOA model is represented as D_o^{besfea} . Then, the optimally selected feature model from the query images are represented as q_u^{besfea} .

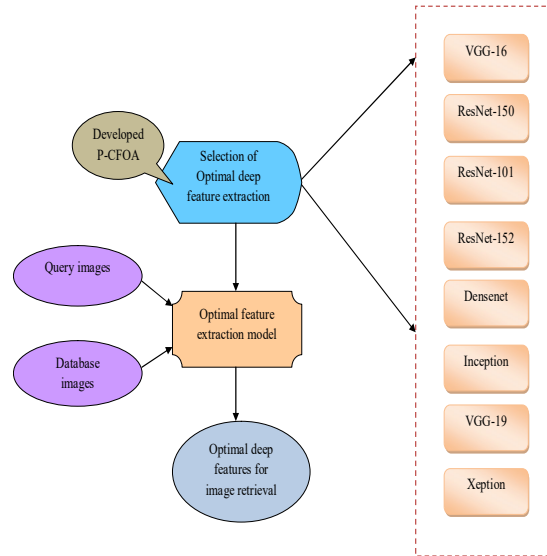


Figure 4: Optimal Deep Feature Selection Model for CBIR framework

6. RESULTS AND DISCUSSIONS

6.1 Experimental Setup

The developed CBIR framework on the basis of the weighted multi-similarity function using the developed P-CFOA was implemented in python. Here, the developed model's performance was compared to the traditional models like VGG-16 [30], VGG-19 [30], Inception [31] and Xception [32] and algorithms like "Particle Swarm Optimization (PSO) [28], Coyote Optimization Algorithm (COA) [26], Forest Optimization Algorithm (FOA) [27], And Coyote Optimization Algorithm-Grey-Wolf Optimization COA-GWO [29]" based on "F1-score, Precision and Recall". The analysis was done by considering "two datasets" and evaluated the retrieved image performance.

6.2 Retrieved images with query image

Few retrieved query images are provided in Fig. 5, in which the developed P-CFOA attains highly relevant images on the basis of query images.


























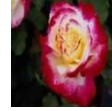


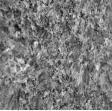
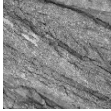














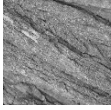
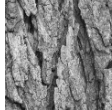



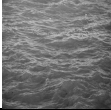


Dataset 1					
Query image-flower					
Retrieved image by PSO					
Retrieved image by COA					
Retrieved image by FOA					
Retrieved image by COA-GWO					
Retrieved image by developed P-CFOA					
Dataset 2					
Query image-bark					
Retrieved image by PSO					
Retrieved image by COA					
Retrieved image by FOA					
Retrieved image by COA-GWO					
Retrieved image by developed P-CFOA					

Figure 5: Retrieved query images using proposed and various existing algorithms

6.3 Retrieved images with query image

The analysis on the potentiality of developed CBIR framework over various algorithms for both

dataset 1 and dataset 2 are represented in Fig 6 and Fig 7, respectively. It was observed that, for datasets 1 and 2, the developed P-CFOA approach attains greater efficiency than other traditional

models. This proves developed model is improving the performance.

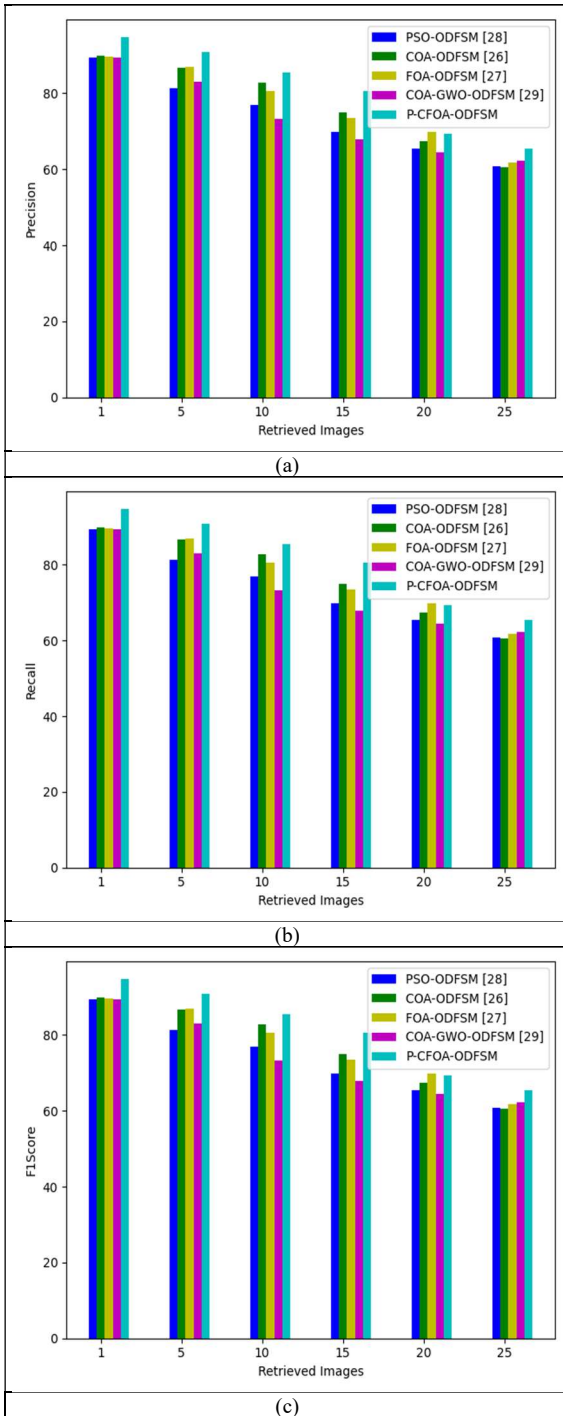


Figure 6: Analysis on the developed CBIR framework with weighted multi-similarity function over various algorithms for dataset 1 in terms of (a) Precision, (b) Recall, and (c) F1-score”

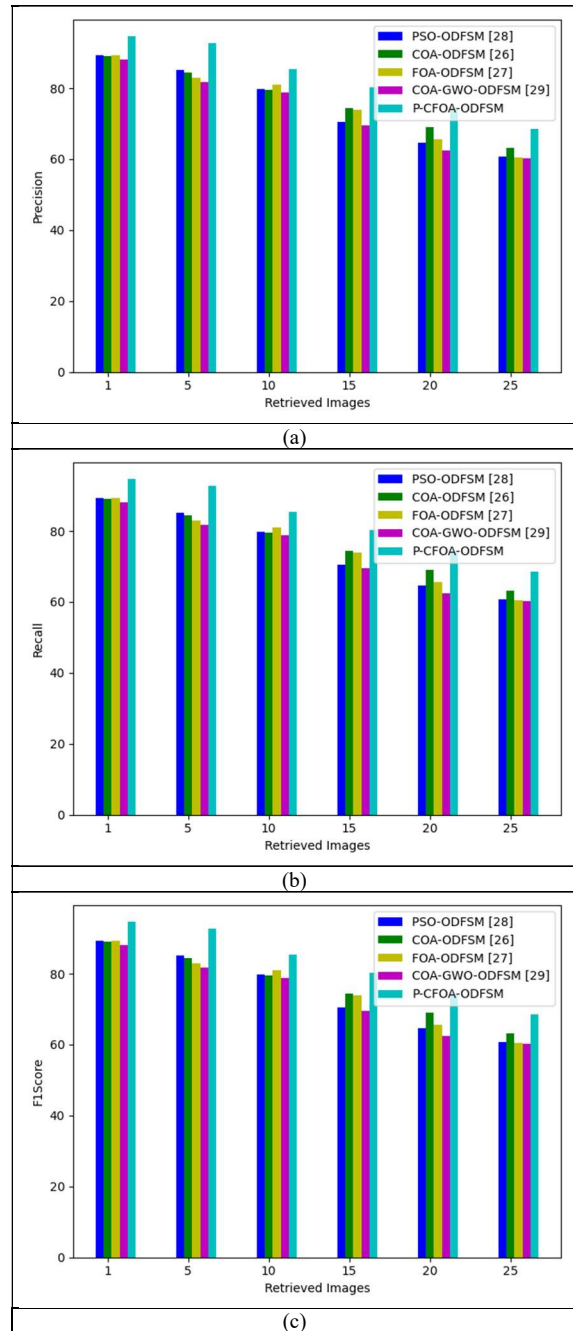


Figure 7: Analysis on the developed CBIR framework with weighted multi-similarity function over various algorithms “for dataset 2 in terms of (a) Precision, (b) Recall, and (c) F1-score”

6.4 Investigation on developed CBIR framework with various classifiers

The analysis on suggested weighted multi-similarity based CBIR framework is valuated with two datasets by comparing various classifiers as

represented in Fig 8 and Fig 9, respectively. The CBIR model utilizing proposed P-CFOA based on precision is 11.3%, 9.2%, and 6.5% superior accuracy to the “VGG-16, Inception v3 and Xception”, respectively.

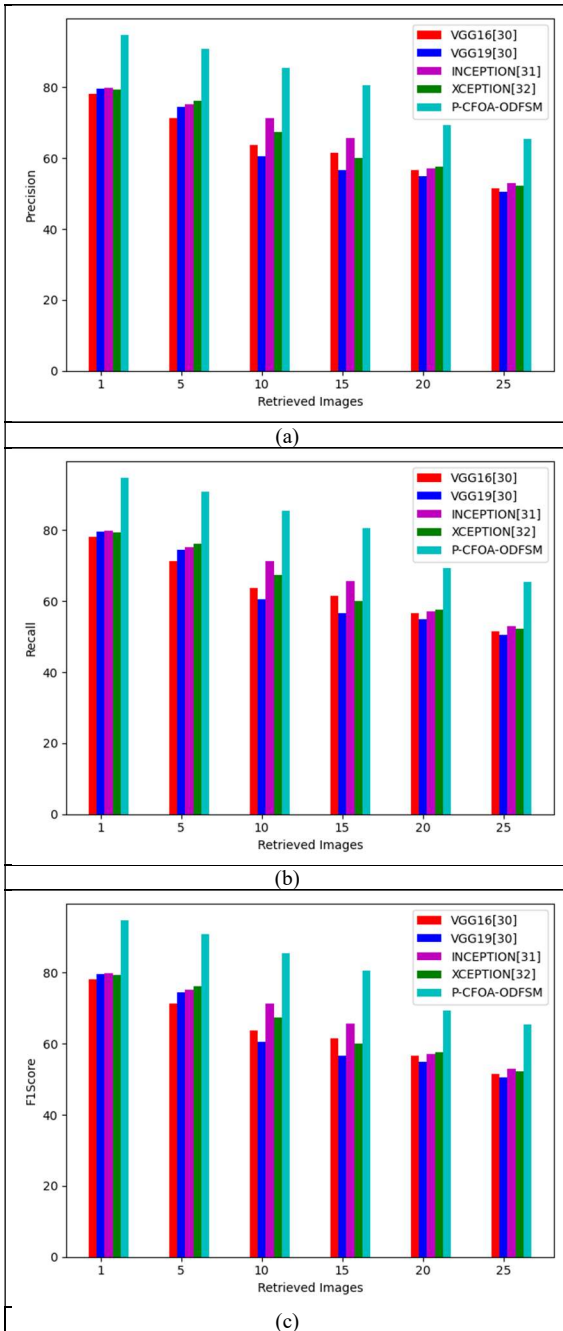


Figure 8: Analysis on the developed CBIR framework with weighted multi-similarity function over various classifiers “for dataset 1 in terms of (a) Precision, (b) Recall, and (c) F1-score”

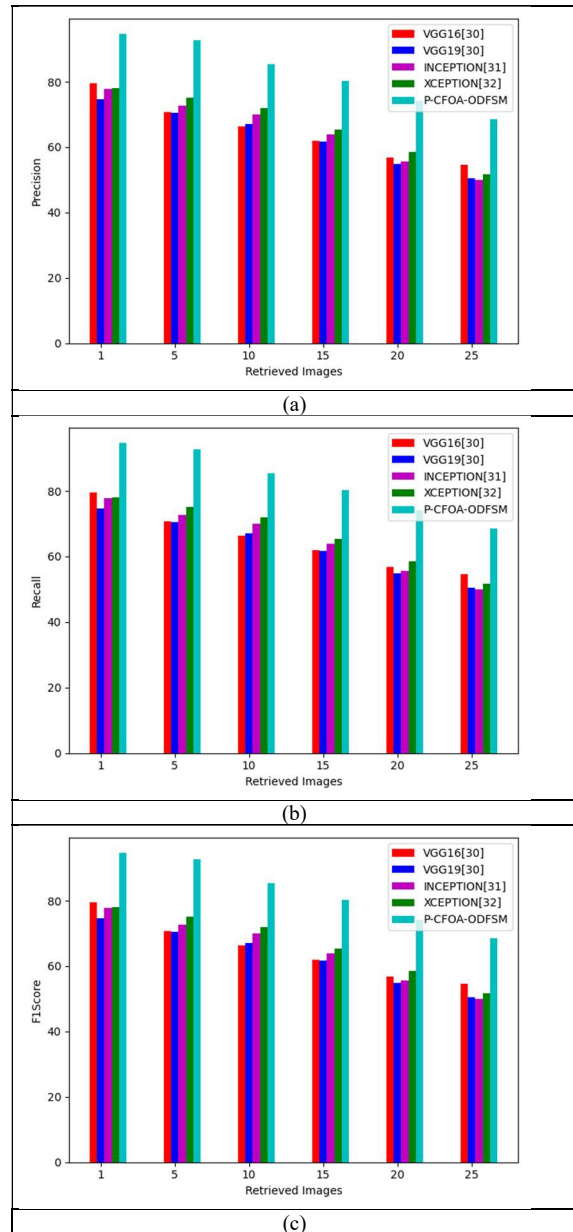


Figure 9: Analysis on the developed CBIR framework with weighted multi-similarity function over various classifiers “for dataset 2 in terms of (a) Precision, (b) Recall, and (c) F1-score”

6.5 Overall Performance evaluation over various algorithms

The comparative analysis between various algorithms is carried out during the evaluation. The analysis takes place between several algorithms in terms of “precision, recall and F1-score” for dataset 1 in Table-2, Table-3, Table 4 and for dataset 2 in, Table 5, Table 6 and Table 7, respectively.

Table 2: Comparative analysis of CBIR framework with various algorithms in terms of precision on dataset 1

QUERY	PSO-ODFSM [28]	COA-ODFSM [26]	FOA-ODFSM [27]	COA-GWO-ODFSM [29]	P-CFOA-ODFSM
1	53.59185	68.83464	68.55162	72.75082	75.11865
2	58.9831	55.93357	68.81432	70.07099	74.45897
3	77.27839	57.86777	51.91694	74.46487	78.1877
4	66.83786	50.97069	64.9021	54.74221	75.95455
5	78.7084	63.74505	77.27295	76.71894	78.9175
6	65.50538	76.39116	50.17504	59.09057	76.64522
7	61.53352	50.3029	75.55347	78.00548	78.00548
8	57.05494	57.92814	69.81463	54.78225	75.11865
9	79.31267	64.2171	73.0455	66.50173	79.31267

Table 3: Comparative analysis of CBIR framework with various algorithms in terms of recall on dataset 1

QUERY	PSO-ODFSM [28]	COA-ODFSM [26]	FOA-ODFSM [27]	COA-GWO-ODFSM [29]	P-CFOA-ODFSM
1	74.28927	72.429	66.07178	69.18507	77.79282
2	77.39506	66.05091	78.55069	71.8513	79.60845
3	62.87305	74.20562	63.06076	61.78156	77.27959
4	65.00896	76.98809	68.19914	60.98798	77.93529
5	75.93614	70.47891	60.60974	62.89863	78.33219
6	65.58892	73.72067	73.62348	66.24528	75.21621
7	76.4524	71.51714	73.40053	74.47942	79.09317
8	77.12975	64.20559	66.80155	67.32573	78.5448
9	61.15824	62.34858	71.94745	64.10746	74.33174

Table 4: Comparative analysis of CBIR framework with various algorithms in terms of f1-score on dataset 1

QUERY	PSO-ODFSM [28]	COA-ODFSM [26]	FOA-ODFSM [27]	COA-GWO-ODFSM [29]	P-CFOA-ODFSM
1	71.36508	60.97609	55.25045	53.27295	73.07924
2	55.31024	62.48319	55.21391	50.06596	79.31874
3	75.28132	51.85016	65.84998	59.39117	79.73977
4	62.92305	56.64574	50.69282	77.38429	77.89708
5	59.9507	63.57705	65.53513	60.26609	71.85295
6	72.95786	54.35908	72.66817	77.22585	78.79886
7	54.19011	77.88129	77.50066	52.60863	78.53326
8	58.51913	52.30675	59.61286	63.8598	75.28348
9	59.62031	67.25782	60.51251	62.65557	79.76775

Table 5: Comparative analysis of CBIR framework with various algorithms in terms of precision on dataset 2

QUERY	PSO-ODFSM [28]	COA-ODFSM [26]	FOA-ODFSM [27]	COA-GWO-ODFSM [29]	P-CFOA-ODFSM
1	62.99413	53.04637	69.58206	54.53064	78.94912
2	68.44124	56.77858	76.67667	59.6194	76.67667
3	64.95771	63.51658	50.09354	57.23731	79.08611
4	60.33065	52.92754	75.2874	70.6507	75.2874
5	61.43058	61.07593	69.14562	79.41727	79.41727
6	60.80227	54.62046	65.3114	64.91106	71.8225
7	50.93182	55.26646	56.36562	62.27664	78.00906
8	78.06291	68.30105	54.62357	57.47769	78.06291
9	72.76282	68.48678	62.01619	61.71678	75.88008

Table 6: Comparative analysis of CBIR framework with various algorithms in terms of recall on dataset 2

QUERY	PSO-ODFSM [28]	COA-ODFSM [26]	FOA-ODFSM [27]	COA-GWO-ODFSM [29]	P-CFOA-ODFSM
1	70.22366	66.29351	77.78243	69.95398	79.99308
2	69.49073	69.86128	65.22792	62.95993	78.66123
3	63.50537	74.03419	64.89646	73.5092	74.52041
4	75.14825	78.70577	75.02405	67.48616	79.21765
5	66.40414	63.9673	67.81711	71.24271	78.08692
6	72.47297	68.03679	60.41699	73.09854	77.60235
7	74.03414	76.1237	66.92677	66.49411	78.0677
8	63.1126	62.16405	65.77918	67.84193	79.81927
9	69.69877	61.07524	78.99389	60.15544	79.95921

Table 7: Comparative analysis of CBIR framework with various algorithms in terms of f1-score on dataset 2

QUERY	PSO-ODFSM [28]	COA-ODFSM [26]	FOA-ODFSM [27]	COA-GWO-ODFSM [29]	P-CFOA-ODFSM
1	58.55905	51.27551	53.00861	58.24206	69.61209
2	68.09987	57.82567	58.92351	73.86871	75.59048
3	50.27134	62.59242	57.16325	56.99454	69.93438
4	67.88259	77.17111	70.32592	58.92211	77.67438
5	73.04911	56.25787	77.89526	52.94333	79.50991
6	54.11617	59.15574	63.63364	50.86042	79.98265
7	61.61279	70.25012	64.69702	68.84214	79.19764
8	68.81881	76.62497	52.74923	51.1027	79.88528
9	75.08853	59.91405	61.14527	64.32617	78.33669

6.6 Overall Investigation on various existing retrieval methods

The comparative analysis on the retrieved images with various classifiers is carried out in terms of

“precision, recall and f-1 score” for dataset 1 and presented in Table 8, Table 9, and Table 10 and for dataset 2 presented in Table 11, Table 12 and Table 13, respectively.

Table 8: Comparative analysis of CBIR framework with existing retrieval methods in terms of precision on dataset 1

QUERY	VGG16 [30]	VGG19 [30]	INCEPTION [31]	XCEPTION [32]	P-CFOA-ODFSM
1	63.21873	50.64658	74.45233	59.65812	77.90388
2	55.95184	74.45897	69.46657	62.6887	74.45897
3	56.54698	78.1877	51.93751	71.87252	78.1877
4	60.2552	54.71652	75.95455	50.86444	75.95455
5	55.54891	59.3243	69.31676	78.9175	78.9175
6	72.11225	76.64522	61.27297	63.77875	76.64522
7	59.19603	59.5104	62.40686	65.13647	78.00548
8	60.3193	65.54296	68.86598	54.87444	75.11865
9	50.73667	50.59647	56.79424	56.82417	79.31267

Table 9: Comparative analysis of CBIR framework with existing retrieval methods in terms of recall on dataset 1

QUERY	VGG16 [30]	VGG19 [30]	INCEPTION [31]	XCEPTION [32]	P-CFOA-ODFSM
1	60.23796	74.41011	72.65464	74.54709	77.79282
2	70.42538	68.10852	69.24858	79.44859	79.60845
3	68.83236	60.96241	64.81044	67.90954	77.27959
4	64.91686	62.59457	71.33926	64.41287	77.93529
5	67.22793	70.78928	67.58373	64.16582	78.33219
6	65.62609	74.59978	66.86256	71.43859	75.21621
7	68.90758	62.66081	72.62389	67.78894	79.09317
8	64.7443	73.67303	73.0172	77.88768	78.5448
9	64.46268	62.18069	68.98084	69.63066	74.33174

Table 10: Comparative analysis of CBIR framework with existing retrieval methods in terms of f1-score on dataset 1

QUERY	VGG16 [30]	VGG19 [30]	INCEPTION [31]	XCEPTION [32]	P-CFOA-ODFSM
1	61.01082	53.3831	54.10295	72.7512	73.07924
2	53.69965	59.18546	58.52285	79.14912	79.31874
3	58.61267	58.83739	55.79023	52.6212	79.73977
4	73.4252	74.08592	60.64896	50.56971	77.89708
5	56.26645	52.47727	61.79094	56.40458	71.85295
6	68.9329	50.25927	76.12482	51.28528	78.79886
7	76.68009	63.79426	55.43718	78.3988	78.53326
8	62.72153	66.66883	58.53378	59.31673	75.28348
9	51.84529	63.85295	57.29634	65.28221	79.76775

Table 11: Comparative analysis of CBIR framework with existing retrieval methods in terms of precision on dataset 2

QUERY	VGG16 [30]	VGG19 [30]	INCEPTION [31]	XCEPTION [32]	P-CFOA-ODFSM
1	64.69555	73.50436	64.92542	68.5677	78.94912
2	56.8353	55.0595	60.11568	75.5501	76.67667
3	78.7669	79.08611	55.67832	64.65274	79.08611
4	65.95545	57.58257	65.4209	54.42041	75.2874
5	64.67537	66.92426	77.1326	67.62431	79.41727
6	52.46224	69.72275	70.67362	71.8225	71.8225
7	61.64994	78.00906	62.84004	53.18218	78.00906
8	77.04725	74.31041	56.64047	56.40474	78.06291
9	55.19596	60.12803	58.7012	75.88008	75.88008

Table 12: Comparative analysis of CBIR framework with existing retrieval methods in terms of recall on dataset 2

QUERY	VGG16 [30]	VGG19 [30]	INCEPTION [31]	XCEPTION [32]	P-CFOA-ODFSM
1	74.09571	67.11244	75.80684	61.86741	79.99308
2	73.53541	64.36737	76.58791	67.73324	78.66123
3	71.13854	65.50534	65.88788	64.26024	74.52041
4	65.87579	74.21202	76.27294	72.50026	79.21765
5	73.15107	67.01589	62.06053	68.90025	78.08692
6	70.39455	65.85394	76.04675	65.59408	77.60235
7	67.28467	64.91615	61.18584	73.62433	78.0677
8	65.45416	63.85508	68.45435	75.04318	79.81927
9	69.16693	78.46143	75.55714	78.46976	79.95921

Table 13: Comparative analysis of CBIR framework with existing retrieval methods in terms of precision on dataset 2

QUERY	VGG16 [30]	VGG19 [30]	INCEPTION [31]	XCEPTION [32]	P-CFOA-ODFSM
1	60.58027	57.99478	50.28058	54.65331	69.61209
2	64.59859	63.14729	55.73435	53.45347	75.59048
3	62.08236	61.06048	53.51274	61.12088	69.93438
4	69.1181	72.65296	51.64058	51.12834	77.67438
5	62.78105	56.41092	78.09132	59.79567	79.50991
6	69.51631	65.65011	52.46807	64.06802	79.98265
7	51.50059	63.7524	50.20608	72.33273	79.19764
8	54.30725	51.92667	66.47817	78.09414	79.88528
9	76.44937	69.92549	67.74879	75.78569	78.33669

In this model, various types of images were collected from two datasets. These collected images were used in the process of deep feature extraction model, which was carried out by utilizing “VGG-16, VGG-19, Inception, Xception, ResNet-150, ResNet-101, ResNet-152 and Densenet” networks for extraction of dataset images along with the query images.

The performance of pertained models such as VGG-16, VGG-19, Inception, and Xception, as well as the proposed model, is compared when used to extract features and retrieve 25 images that are most similar to a given query image from the given dataset. Precision, recall, and f1 score are the metrics used for comparison and the results are presented in the above tables. The depth and quantity of completely connected nodes in the VGG-16 and VGG-19 models make them heavy models [2, 5, 32]. As a result, they demand high levels of computational power and additional memory. But the proposed model requires less memory due to the use of optimal selection

strategy. In image retrieval, our model outperforms VGG-based models despite its high computational cost. The memory requirements of the Inception and Xception models are lower than those of the VGG-16 and VGG-19 models. However, in terms of image retrieval accuracy, the Inception [30] and Xception [31] models perform 2% and 3% lesser than our model, respectively. This shows that the proposed model outperforms the current models.

Apart from the generalization of training data problems, full visual perception is other key research area. Humans can infer object-to-object relationships, object connectivity in the image from segment-to-whole, object properties, and the layout of a scene in addition to identifying objects in a given image. Developing a deep understanding of images is beneficial for performance improvement of modern applications, which often require information other than identifying the object and its location in the image. This exercise requires not only the vision of the image, but also the cognitive knowledge of the real world. This is a limitation of

the proposed work. In future work, we would like to address this issue. Beside this, even though the results are better than existing models, the process takes longer time as the size of the image database grows. In the future, however, a light weighted and trimmed model for image retrieval needs to be developed that can also be used in mobile applications.

7. CONCLUSION

A novel CBIR framework was established in the paper for attaining enhanced results in retrieval of images. In this model, various types of images were collected from two datasets. These collected images were used in the process of deep feature extraction model, which was carried out by utilizing “VGG-16, VGG-19, Inception, Xception, ResNet-150, ResNet-101, ResNet-152 and Densenet” networks for extraction of dataset images along with the query images. Here, new developed P-CFOA was used for the selecting the deep feature model to obtain optimal model. The gathered images from database and query images were restored in the feature library. Then, the process of utilizing the weighted multi-similarity function is carried out by considering three similarity metrics known as “cosine, Euclidean and Jaccard”. Then, three weight functions was considered in each similarity metrics and the weights were optimized by utilizing developed P-FOA for obtaining optimal weighted multi-similarity function. The image comprises of minimum similarity during the comparison of database and query images were attained. By the performance evaluation, the effectiveness and efficiency of deep feature extraction model by utilizing the developed P-CFOA were obtained 11.3%, 9.2% and 6.5% higher accuracy than the “VGG-16, Inception v3 and Xception” models for dataset 1 by considering the retrieved image count as 25. Finally, the evaluations have determined that the developed CBIR framework attained greater accuracy than other traditional image retrieval models.

The novelty in this work is to use of P-CFOA for selecting the optimal features, also using the weighted multi-similarity between the extracted features of database images and query image. The proposed model only works on content-based image retrieval. It has not used cognitive knowledge to further enhance the image retrieval process. Beside this, even though the results are better than existing models, the process takes longer time as the size of the image database grows.

In the future, however, a light weighted and trimmed model needs to be developed. So that it can also be utilized in mobile applications.

REFERENCES:

- [1] P. Liu, J. Guo, C. Wu and D. Cai, "Fusion of Deep Learning and Compressed Domain Features for Content-Based Image Retrieval," *IEEE Transactions on Image Processing*, vol. 26, no. 12, pp. 5706-5717, Dec. 2017.
- [1] Z. N. K. Swati et al., "Content-Based Brain Tumor Retrieval for MR Images Using Transfer Learning," *IEEE Access*, vol. 7, pp. 17809-17822, 2019.
- [2] F. Mustafic, I. Prazina and V. Ljubovic, "A New Method for Improving Content-Based Image Retrieval using Deep Learning," *XXVII International Conference on Information, Communication and Automation Technologies (ICAT)*, 2019.
- [3] Ahmad, F., Ahmad, T, "Content Based Image Retrieval System Based on Deep Convolution Neural Network Model by Integrating Three-Fold Geometric Augmentation", *Opt. Mem. Neural Networks*, vol.30, pp.236–249, 2021.
- [4] Agrawal, S., Chowdhary, A., Agarwala, S, "Content-based medical image retrieval system for lung diseases using deep CNNs", *Int. j. inf. tecnol*, 2022.
- [5] Desai.P, Pujari.J, Sujatha, C, "Hybrid Approach for Content-Based Image Retrieval using VGG16 Layered Architecture and SVM: An Application of Deep Learning", *SN COMPUT. SCI*, vol.2, pp.170, 2021.
- [6] Tuyet, V.T.H., Binh, N.T., Quoc, N.K, "Content Based Medical Image Retrieval Based on Salient Regions Combined with Deep Learning", *Mobile Netw Appl*, vol.26, pp.1300–1310, 2021.
- [7] Y. YOSHINOBU et al., "Deep Learning Method for Content-Based Retrieval of Focal Liver Lesions Using Multiphase Contrast-Enhanced Computer Tomography Images," *IEEE International Conference on Consumer Electronics (ICCE)*, 2020.
- [8] D. Xu, S. Yan, D. Tao, S. Lin and H. Zhang, "Marginal Fisher Analysis and Its Variants for Human Gait Recognition and Content- Based Image Retrieval," *IEEE Transactions on Image Processing*, vol. 16, no. 11, pp. 2811-2821, Nov. 2007.
- [9] G. Paschos, I. Radev and N. Prabakar, "Image content-based retrieval using

- chromaticity moments," *IEEE Transactions on Knowledge and Data Engineering*, vol. 15, no. 5, pp. 1069-1072, Sept.-Oct. 2003.
- [10] Bin Zhu, M. Ramsey and Hsinchun Chen, "Creating a large-scale content-based airphoto image digital library," *IEEE Transactions on Image Processing*, vol. 9, no. 1, pp. 163-167, Jan. 2000.
- [11] A. Preethy Byju, B. Demir and L. Bruzzone, "A Progressive Content-Based Image Retrieval in JPEG 2000 Compressed Remote Sensing Archives," *IEEE Transactions on Geoscience and Remote Sensing*, vol. 58, no. 8, pp. 5739-5751, Aug. 2020.
- [12] J. Zhang and L. Ye, "Content Based Image Retrieval Using Unclean Positive Examples," *IEEE Transactions on Image Processing*, vol. 18, no. 10, pp. 2370-2375, Oct. 2009.
- [13] R. Rahmani, S. A. Goldman, H. Zhang, S. R. Cholleti and J. E. Fritts, "Localized Content-Based Image Retrieval," *IEEE Transactions on Pattern Analysis and Machine Intelligence*, vol. 30, no. 11, pp. 1902-1912, Nov. 2008.
- [14] G. Carneiro, A. B. Chan, P. J. Moreno and N. Vasconcelos, "Supervised Learning of Semantic Classes for Image Annotation and Retrieval," *IEEE Transactions on Pattern Analysis and Machine Intelligence*, vol. 29, no. 3, pp. 394-410, March 2007.
- [15] J. Basak, K. Bhattacharya and S. Chaudhury, "Multiple Exemplar-Based Facial Image Retrieval Using Independent Component Analysis," *IEEE Transactions on Image Processing*, vol. 15, no. 12, pp. 3773-3783, Dec. 2006.
- [16] I. El-Naqa, Yongyi Yang, N. P. Galatsanos, R. M. Nishikawa and M. N. Wernick, "A similarity learning approach to content-based image retrieval: application to digital mammography," *IEEE Transactions on Medical Imaging*, vol. 23, no. 10, pp. 1233-1244, Oct. 2004.
- [17] M. M. Rahman, P. Bhattacharya and B. C. Desai, "A Framework for Medical Image Retrieval Using Machine Learning and Statistical Similarity Matching Techniques With Relevance Feedback," *IEEE Transactions on Information Technology in Biomedicine*, vol. 11, no. 1, pp. 58-69, Jan. 2007.
- [18] A. W. M. Smeulders, M. Worring, S. Santini, A. Gupta and R. Jain, "Content-based image retrieval at the end of the early years," *IEEE Transactions on Pattern Analysis and Machine Intelligence*, vol. 22, no. 12, pp. 1349-1380, Dec. 2000.
- [19] Wei Jiang, Guihua Er, Qionghai Dai and Jinwei Gu, "Similarity-based online feature selection in content-based image retrieval," *IEEE Transactions on Image Processing*, vol. 15, no. 3, pp. 702-712, March 2006.
- [20] Junqing Chen, T. N. Pappas, A. Mojsilovic and B. E. Rogowitz, "Adaptive perceptual color-texture image segmentation," *IEEE Transactions on Image Processing*, vol. 14, no. 10, pp. 1524-1536, Oct. 2005.
- [21] R. Krishnapuram, S. Medasani, Sung-Hwan Jung, Young-Sik Choi and R. Balasubramaniam, "Content-based image retrieval based on a fuzzy approach," *IEEE Transactions on Knowledge and Data Engineering*, vol. 16, no. 10, pp. 1185-1199, Oct. 2004.
- [22] M. Saadatmand-Tarzan and H. A. Moghaddam, "A Novel Evolutionary Approach for Optimizing Content-Based Image Indexing Algorithms," *IEEE Transactions on Systems, Man, and Cybernetics, Part B (Cybernetics)*, vol. 37, no. 1, pp. 139-153, Feb. 2007.
- [23] B. Ko and H. Byun, "FRIP: a region-based image retrieval tool using automatic image segmentation and stepwise Boolean AND matching," *IEEE Transactions on Multimedia*, vol. 7, no. 1, pp. 105-113, Feb. 2005.
- [24] E. Aptoula and S. Lefevre, "Morphological Description of Color Images for Content-Based Image Retrieval," *IEEE Transactions on Image Processing*, vol. 18, no. 11, pp. 2505-2517, Nov. 2009.
- [25] ZhiYuan, WeiqingWang, HaiyunWang, and AbdullahYildizbasi, "Developed Coyote Optimization Algorithm and its application to optimal parameters estimation of PEMFC model", *Energy Reports*, vol.6, pp.1106-1117, November 2020.
- [26] Manizheh Ghaemi, and Mohammad-RezaFeizi-Derakhshi, "Forest Optimization Algorithm", *Expert Systems with Applications*, vol.41, no.15, pp.6676-6687, November 2014.
- [27] M. Broilo and F. G. B. De Natale, "A Stochastic Approach to Image Retrieval Using Relevance Feedback and Particle Swarm Optimization," *IEEE Transactions on Multimedia*, vol. 12, no. 4, pp. 267-277, June 2010.
- [28] Abhishek Kumar, SwarnAvinash Kumar, Vishal Dutt, Ashutosh KumarDubey and Vicente García Díaz, "IoT-based ECG monitoring for arrhythmia classification using Coyote Grey Wolf optimization-based deep learning CNN

- classifier", *Biomedical Signal Processing and Control*, Vol.76, pp.103638, July 2022.
- [29] M.Toğaçar, B.Ergen, Z.Cömert and F.Özyurt, "A Deep Feature Learning Model for Pneumonia Detection Applying a Combination of mRMR Feature Selection and Machine Learning Models", *IRBM*, Vol.41, Issue.4, pp.212-222, August 2020.
- [30] Z. Yue, J. Luo, F. Husheng, F. Shao and Z. Ranzhi, "Study on the Identification Method of Human Upper Limb Flag Movements Based on Inception-ResNet Double Stream Network," *IEEE Access*, vol. 9, pp. 85764-85784, 2021.
- [31] S. Roopashree and J. Anitha, "DeepHerb: A Vision Based System for Medicinal Plants Using Xception Features," *IEEE Access*, vol. 9, pp. 135927-135941, 2021.
- [32] Narin, A., Kaya, C. & Pamuk, Z, "Automatic detection of coronavirus disease (COVID-19) using X-ray images and deep convolutional neural networks", *Pattern Anal Applic*, vol.24, pp.1207–1220, 2021.
- [33] Wang, Shuihua & Zhang, Yu-Dong, "DenseNet-201-Based Deep Neural Network with Composite Learning Factor and Precomputation for Multiple Sclerosis Classification", *ACM Transactions on Multimedia Computing Communications and Applications*, vol.16, pp.1-19, 2020.